

Signals of new physics in global event properties in pp collisions in the TeV energy domain: rapidity intervals

A. Giovannini, R. Ugoccioni

Dipartimento di Fisica Teorica and INFN – Sezione di Torino Via P. Giuria 1, 10125 Torino, Italy

Received: 3 March 2004 /

Published online: 23 July 2004 – © Springer-Verlag / Società Italiana di Fisica 2004

Abstract. The study of possible new physics signals in global event properties in pp collisions in the TeV energy domain is extended from full phase-space to rapidity intervals experimentally accessible at LHC. The elbow structure in the total multiplicity distribution predicted in full phase-space is clearly present also in restricted rapidity intervals, leading to very strong charged particle correlations. It is also found that energy densities comparable to those reached in heavy ion collisions at RHIC could be attained in pp collisions at LHC.

Introduction

The search for signals of new physics in global event properties in pp collisions at LHC in the framework of the weighted superposition mechanism of different classes of minimum bias events as components led us to explore the possibility of the existence at 14 TeV c.m. energy of a new class of events [1]. The aim of the present paper is to extend our study from full phase-space (FPS) to pseudo-rapidity intervals which will become experimentally accessible with the LHC detectors.

The paper is organised as follows. In Sect. 1 are summarised results of [2] on general properties of soft and semi-hard components in pseudo-rapidity intervals in extrapolated scenarios based on the knowledge of the 10^2 to 10^3 GeV energy domain. In Sect. 2 the existence at 14 TeV c.m. energy in pp collisions of a third class of events in addition to the soft and semi-hard ones is postulated following our findings on the same class in FPS and its general properties in pseudo-rapidity intervals are discussed. For completeness, a comparison with Pythia Monte Carlo calculation results is performed where appropriate.

1 Antecedents: global properties in full phase-space

In [2] the total n -charged particle multiplicity distribution in pseudo-rapidity intervals $|\eta| < \eta_c$ as a function of c.m. energy \sqrt{s} was written as follows:

$$P_n(\eta_c, \sqrt{s}) = \alpha_{\text{soft}}(\sqrt{s}) P_n^{\text{PaNB}}(\bar{n}_{\text{soft}}(\eta_c, \sqrt{s}), k_{\text{soft}}(\eta_c, \sqrt{s})) + (1 - \alpha_{\text{soft}}(\sqrt{s})) P_n^{\text{PaNB}}(\bar{n}_{\text{sh}}(\eta_c, \sqrt{s}), k_{\text{sh}}(\eta_c, \sqrt{s})), \quad (1)$$

where $P_n^{\text{PaNB}}(\bar{n}, k)$ are Pascal (negative binomial) multiplicity distributions with characteristic parameters \bar{n} , the average charged multiplicity, and k , related to the dispersion D by $k^{-1} = (D^2 - \bar{n})/\bar{n}^2$, in the pseudo-rapidity interval $|\eta| < \eta_c$ at c.m. energy \sqrt{s} for the soft and semi-hard components, and α_{soft} is the fraction of soft events with respect to the total number of events. One defines next the clan structure parameters [3]: the average number of clans, $\bar{N} = k \ln(1 + \bar{n}/k)$, and the average number of particles per clan, $\bar{n}_c = \bar{n}/\bar{N}$. The most appealing result has been the decrease of the average number of clans of the semi-hard component $\bar{N}_{\text{sh}}(\eta_c)$ at fixed η_c as \sqrt{s} increases (already seen in FPS [4]) both in the strong-KNO-scaling-violating scenario (where $k_{\text{total}}^{-1} \simeq \ln s$) and in the QCD-inspired one (where $k_{\text{sh}}^{-1} \simeq a - b/\sqrt{\ln s}$, with a and b both > 0 , determined by interpolating low energy data [2]), together with the corresponding increase of the average number of particles per clan. In addition, the decrease of $\bar{N}_{\text{sh}}(\eta_c)$ was found to be quicker in the strong-KNO-scaling-violating scenario than in the QCD-inspired one and more pronounced in larger intervals than in smaller ones.

Finally the average number of clans increased with the width of the rapidity interval; the average number of particles per clan $\bar{n}_{c,\text{sh}}$ also increased with the width of the rapidity interval and, contrary to \bar{N}_{sh} , increased also with c.m. energy.

This situation raised intriguing questions, on when the asymptotic limit $\bar{N}_{\text{sh}} \rightarrow 1$ will be reached and on the consequences of its eventual earlier occurrence, say at LHC energy.

In [1] we concluded that an early occurrence of the limit $\bar{N}_{\text{sh}} \rightarrow 1$ in FPS is of particular interest and leads in our framework to the onset of a new class of events, described by an NBD with $\bar{N}_{\text{th}} = 1$, accounting for 1-3

percent of the total event sample¹, with quite remarkable properties controlled by $k_{\text{th}} < 1$, the effective benchmark of the new class of events.

In particular are expected:

a) very strong forward-backward (FB) multiplicity correlations (the FB multiplicity correlations strength is close to its maximum, $b_{\text{FB}} \sim 1$) with leakage parameter controlling the flow of particles from one hemisphere to the opposite one [5] $p \sim 1/2$, again its maximum value;

b) an enhancement of two-particle correlations determined by the very large value of k_{th}^{-1} ;

c) a characteristic elbow structure in P_n^{total} for large n and a narrow peak for n close to zero. Both trends are consequences of the log-convex gamma shape of the n -charged particles multiplicity distribution of the new component which shows a high peak at very low multiplicities and a very slow decrease for large ones, a general behaviour to be contrasted with Pythia Monte Carlo calculation predictions, which show at 14 TeV a second shoulder to be added to the first one already seen in the 10^2 to 10^3 GeV energy domain.

The situation is summarised in Fig. 1 within the framework of the weighted superposition mechanism of the three classes of events and in Fig. 2 for Pythia Monte Carlo predictions. It should be noticed that the total MD also in the case of Pythia can be fitted in terms of the superposition of three negative binomial distributions (NBD's) with chi-square per degree of freedom = 107/66. The corresponding characteristic NBD parameters of the two cases are given in Table 1a and 1c respectively. Striking differences between the behaviours of events of the third class, seen just by inspection of Figs. 1 and 2, are shown explicitly in the mentioned tables.

2 Perspectives: global properties in rapidity intervals

Tevatron data seem to favour, among our scenarios, the one based on a strong KNO-scaling violation (i.e., with $k_{\text{total}}^{-1} \simeq \ln s$). In fact it was shown by CDF [6] that, in their data, the component rich in mini-jets violates KNO scaling in small rapidity intervals, although a cut-off at low p_T has been used; in addition, E735 data in FPS [7] show again that the closest scenario is the one mentioned above, although discrepancies with previous UA5 results [8] are noticed in E735 results at lower c.m. energies. Therefore, we decided to discuss in rapidity intervals the case of the strong-KNO-scaling-violating scenario only.

In going from FPS to (pseudo)-rapidity intervals our main concern has been to be consistent with the scenarios explored in FPS. The weight of each component is obviously the same as in FPS. This leads to a particle density which shows an energy-independent plateau around $\eta = 0$ in both the soft and the semihard components, a constant k_{soft} value and a linearly increasing k_{total} . It should be

¹ so as not to affect the overall average charged multiplicity more than 10% [1]

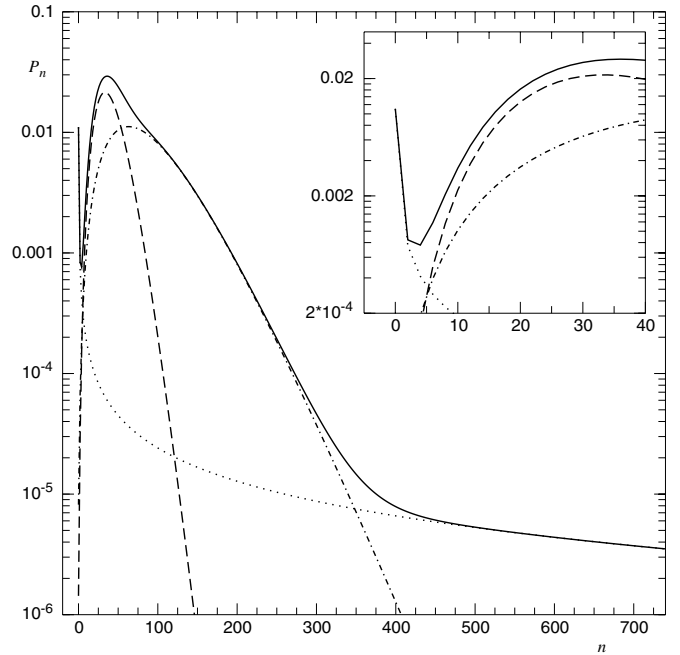


Fig. 1. Full phase-space multiplicity distribution for the scenario described in the text (solid line); the three components are also shown: soft (dashed line), semi-hard (dash-dotted line) and the third (dotted line). The inset shows a magnification of the low-multiplicity peak

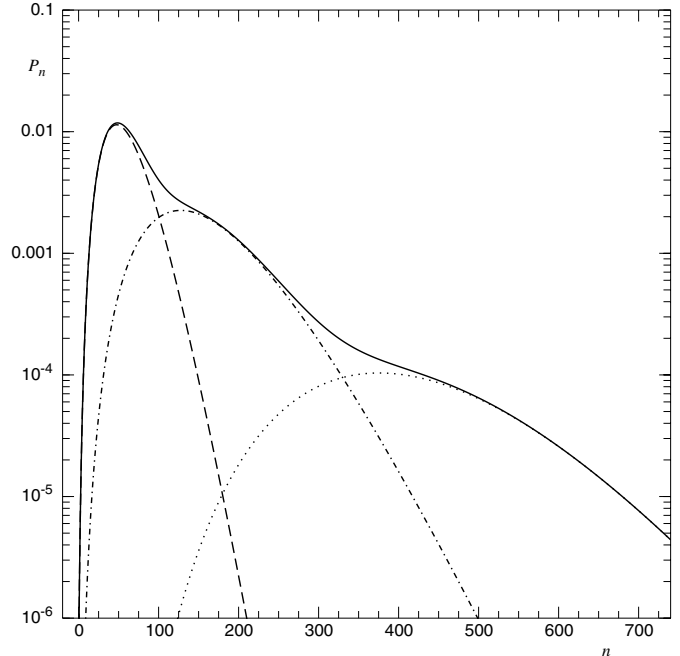


Fig. 2. Three-component negative binomial distribution (NBD) fit to the full phase-space multiplicity distribution predicted by Pythia Monte Carlo calculations at 14 TeV; the three component NBD's are also shown

Table 1. a Parameters for the extrapolated component MD's at 14 TeV in FPS; **b** same as **a**, but in the pseudo-rapidity interval $|\eta| < 0.9$, with the two extreme scenarios: evenly spread over the whole rapidity range (i) and concentrated in the small interval (ii); **c** Parameters of NBD fits to Pythia predictions in FPS; **d** same as **c**, but in the pseudo-rapidity interval $|\eta| < 0.9$. Error values given in **c** and **d** are statistical errors from the fits

a	FPS	%	\bar{n}	k	\bar{N}	\bar{n}_c
	soft	41	40	7.0	13	3.0
	semi-hard	57	87	3.7	12	7.4
	third	2	460	0.12	1	460
b	$ \eta < 0.9$	%	\bar{n}	k	\bar{N}	\bar{n}_c
	soft	41	4.9	3.4	3.0	1.6
	semi-hard	57	14	2.0	4.2	3.4
	third (i)	2	40	0.06	0.39	103
	third (ii)	2	460	0.12	1	460
c	FPS	%	\bar{n}	k	\bar{N}	\bar{n}_c
	first	42 ± 4	52.8 ± 0.2	11 ± 1	19.3 ± 1.4	2.7 ± 0.2
	second	56 ± 4	123 ± 3	2.7 ± 0.2	10.5 ± 0.7	11.7 ± 1.2
	third	≈ 2	468 ± 7	23 ± 3	70 ± 7	6.6 ± 0.6
d	$ \eta < 0.9$	%	\bar{n}	k	\bar{N}	\bar{n}_c
	first	52 ± 7	5.1 ± 0.2	2.8 ± 0.3	2.9 ± 0.1	1.75 ± 0.1
	second	47 ± 7	19.1 ± 1.5	1.9 ± 0.5	4.5 ± 0.7	4.2 ± 0.7
	third	≈ 1	87.7 ± 3.7	11 ± 4	24 ± 5	3.6 ± 0.8

remarked that the plateau of the semihard component is less wide than that of the soft component, but it is higher. See [2] for a detailed discussion on these points.

For the third component, we have allowed for two extreme behaviours: (i) the third component is distributed uniformly over the whole of phase space and (ii) the third component has a very narrow and tall plateau and falls entirely within the interval $|\eta| < 0.9$. These two extremes are represented as a band in the figure. In the first case, the value of k_{th} has again been determined from the asymptotic behaviour of the average number of clans in the second (semihard) component, where it is a fixed fraction of the same quantity in FPS. Results are shown in Fig. 3 and Table 1b.

It should be pointed out that the general trend of P_n vs. n is quite similar to that already seen in FPS: the elbow structure is clearly visible in both extreme cases; on the other hand, the narrow peak at very low multiplicities (also due to the third component) is hidden by the standard peaks of the soft and semi-hard components which are shifted to lower multiplicities than in FPS.

This behaviour is clearly seen in Tables 1a and 1b by comparing \bar{n}_{sh} with \bar{n}_{soft} and k_{sh} with k_{soft} in FPS and in rapidity intervals. In addition it turns out that $\bar{N}_{soft}(FPS)$ is slightly larger than $\bar{N}_{sh}(FPS)$ and $\bar{N}_{soft}(|\eta| < 0.9)$ is slightly smaller than $\bar{N}_{sh}(|\eta| < 0.9)$, but the average number of particles per clan is both in FPS and in $|\eta| < 0.9$ much larger in the semi-hard than in the soft component, a fact which confirms the general trend that semi-hard clans are larger than soft clans.

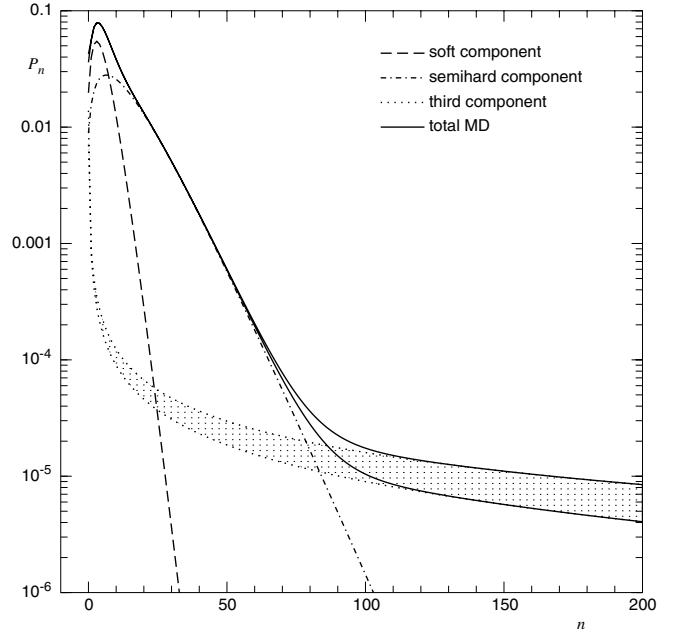


Fig. 3. Multiplicity distribution in $|\eta| < 0.9$ for the scenario described in the text (solid line); the three components are also shown: soft (dashed line), semi-hard (dash-dotted line) and the third (dotted line)

Table 2. Forward-backward multiplicity correlation strength both in our scenarios and in Pythia Monte Carlo calculations

	Pythia		Our scenarios		
	FPS	$ \eta < 0.9$	FPS	$ \eta < 0.9$	
first/soft	0.39 ± 0.01	0.28 ± 0.02	0.41	0.25	
second/semihard	0.53 ± 0.01	0.48 ± 0.01	0.51	0.45	
third	0.91 ± 0.02	0.80 ± 0.04	0.999	0.997	(i)
				0.999	(ii)
total (weighted)	0.75 ± 0.03	0.69 ± 0.05	0.98	0.92	

As far as the third component is concerned, we have the mentioned extreme situations according to our assumptions:

i) a situation in which the single clan is uniformly spread over the whole of phase space (in this case only 39% of the clan is contained within the pseudo-rapidity interval $|\eta| < 0.9$), k_{th} is even much less than 1 ($k_{\text{th}} \sim 0.06$) and $\bar{n}_{\text{th}} \sim 40$.

ii) a situation in which the single clan is fully contained in $|\eta| < 0.9$, i.e., its characteristic parameters are the same as those seen in FPS. It is quite clear that particle density in rapidity in this second case is much higher than in case (i).

In Fig. 4 are shown the three components and their superposition predicted by Pythia at 14 TeV in the interval $|\eta| < 0.9$. We have taken the results from [1], where Pythia version 6.210 [9] was run with default parameters using model 4 with a double Gaussian matter distribution. This set-up gives a reasonable description of lower energy MD data. The same events were then analysed both in FPS

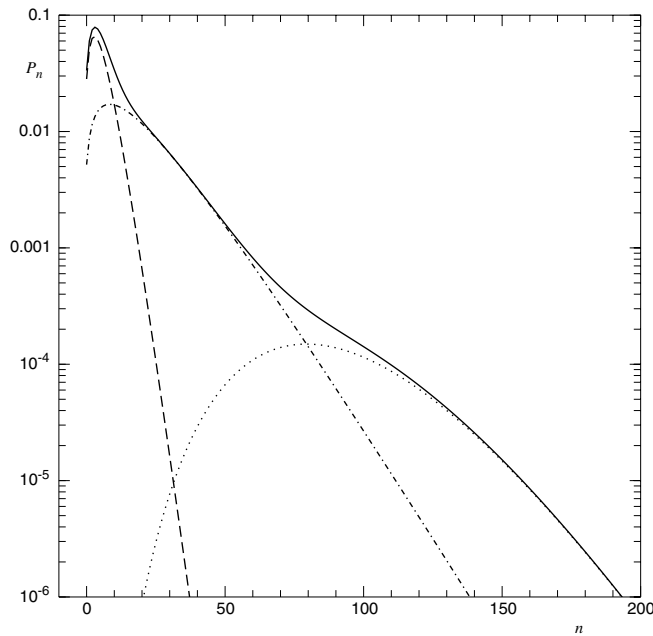


Fig. 4. Three-component NBD fit to the multiplicity distribution in $|\eta| < 0.9$ predicted by Pythia Monte Carlo calculations at 14 TeV; the three component NBD's are also shown

and in the rapidity interval $|\eta| < 0.9$. The MD's thus found have been fitted with the weighted sum of three NBD's (it was not possible to use just two NBD's), which have been taken as the three components. The parameters of the NBD fits can be found in Table 1d ($\chi^2/\text{NDF} = 34/42$).

As in FPS, the behaviour of the tail is completely different from that predicted by our scenarios. It should be noticed that the average number of particle per clan is quite small in all components although the average number of clans increases from the first to the third component suggesting Poissonian MD structure in each component.

Coming to FB multiplicity correlations, it is important to stress that our previous calculations [5] of the correlation strength, b_{FB} , for the two components,

$$b_{\text{FB}} = \frac{\alpha_1 \frac{b_1 D_1^2}{1+b_1} + (1-\alpha_1) \frac{b_2 D_2^2}{1+b_2} + \frac{1}{2} \alpha_1 (1-\alpha_1) (\bar{n}_2 - \bar{n}_1)^2}{\alpha_1 \frac{D_1^2}{1+b_1} + (1-\alpha_1) \frac{D_2^2}{1+b_2} + \frac{1}{2} \alpha_1 (1-\alpha_1) (\bar{n}_2 - \bar{n}_1)^2}, \quad (2)$$

where, for the i -th component, \bar{n}_i is its average multiplicity, D_i its dispersion, b_i its FB correlation strength and α_i its weight, should be extended to accommodate the third one. Accordingly, we derived the following formula for the overall strength for an arbitrary number M of components:

$$b_{\text{FB}} = \frac{\sum_{i=1}^M \alpha_i \frac{b_i D_i^2}{1+b_i} + \frac{1}{2} \sum_{i=1}^M \sum_{j>i}^M \alpha_i \alpha_j (\bar{n}_i - \bar{n}_j)^2}{\sum_{i=1}^M \alpha_i \frac{D_i^2}{1+b_i} + \frac{1}{2} \sum_{i=1}^M \sum_{j>i}^M \alpha_i \alpha_j (\bar{n}_i - \bar{n}_j)^2}. \quad (3)$$

Applied to the three components case, Eq (3) leads to the results shown in Table 2, where the leakage parameter in rapidity intervals has been taken to be the same as in FPS [5]. In particular it is clear that the FB correlation strength for the soft component is quite larger in FPS than in $|\eta| < 0.9$ ($b_{\text{FB,soft}}(\text{FPS}) = 0.41$, $b_{\text{FB,soft}}(|\eta| < 0.9) = 0.25$) and still remains larger in FPS than in $|\eta| < 0.9$ for the semi-hard component ($b_{\text{FB,sh}}(\text{FPS}) = 0.51$, $b_{\text{FB,sh}}(|\eta| < 0.9) = 0.45$), although it is always much larger both in FPS and in $|\eta| < 0.9$ for the semi-hard component than for the soft one. The third component tends to saturate in all cases its maximum value, which is 1. The total FB multiplicity correlation strength resulting from the composition of the contributions of all classes of events is larger in FPS ($b_{\text{FB}} = 0.98$) than in $|\eta| < 0.9$ ($b_{\text{FB}} = 0.92$) but closer to its asymptotic value.

FB correlations in Pythia do not show remarkable differences with respect to our scenarios except in the third

Table 3. Energy density and corresponding parameters for our scenarios and for Pythia Monte Carlo. The volume $V = \pi R^2 \tau$ has been computed with proton radius $R \approx 1.1$ fm and formation time $\tau \approx 1$ fm

a	our scenarios	soft	semi-hard	third (i)	(ii)	total (i)	(ii)
	dn/dy	2.5	7	20	230	10.8	19.2
	$\langle E_T \rangle$ (MeV)	350	500	500	500	500	500
	ε (GeV/fm ³)	0.41	1.6	4.7	54	2.5	4.5
b	Pythia	first	second	third		total	
	dn/dy	2.5	9.5	44		12.5	
	$\langle E_T \rangle$ (MeV)	350	500	500		500	
	ε (GeV/fm ³)	0.41	2.4	10		3.0	

component and in the total MD where they are considerably smaller; in particular the difference with the third component is striking (0.8 Pythia, ≈ 1 our scenarios). Stronger FB correlations at hadron level suggest an extraordinary stronger colour exchange process at parton level in the last case.

In addition, Bjorken formula [10] for the energy density,

$$\varepsilon = \frac{3 \langle E_T \rangle}{2 V} \frac{dn}{dy} \Big|_{y=0}, \quad (4)$$

where $\langle E_T \rangle$ is the average transverse energy per particle, V the collision volume and dn/dy the particle density at mid-rapidity, has been applied in order to compare its predictions on pp collisions with those on nucleus-nucleus collisions. Parameters of the formula and results are shown in Table 3a: dn/dy values correspond to predictions for our scenarios already seen in Table 1; lacking general expectations for the average transverse energy $\langle E_T \rangle$, we used for the soft component the value measured at ISR and, in a conservative way, the value measured by CDF for the other components (to be intended as a lower bound, which leads to lower bounds for the energy density as well).

It should be noticed that:

a) the energy density for the semi-hard component in our scenario at 14 TeV is ≈ 1.6 GeV/fm³, i.e., of the same order of magnitude of that found at AGS at 5.6 GeV in O+Cu collisions ($\varepsilon \approx 1.7$ GeV/fm³).

b) the energy density for the third component in the spread out scenario is 4.7 GeV/fm³, i.e., comparable with the value of ε recently measured at RHIC in Au+Au collisions ($\varepsilon \approx 4.6$ GeV/fm³).

c) the energy density for the third component in the other extreme scenario (high concentration) is ≈ 54 GeV/fm³, even larger, being dn/dy much larger, than the LHC expectations for central Pb+Pb collisions ($\varepsilon \gtrsim 15$ GeV/fm³).

On the other side, Pythia prediction for its third component (see Table 3b) is contained within our extreme predictions, and it is of the same order of magnitude in the other components. Notice that the full minimum bias sample is also intermediate between our scenarios results.

Of course our calculation of ε is only indicative and should be taken with caution. Although the use of Bjorken formula for pp collisions as well as the choice of param-

eters is rather doubtful, we consider our results quite stimulating because they suggest the possibility that the same characteristic behaviour of many observables seen at RHIC energies in AA collisions could be reproduced at LHC in pp collisions.

The implications of the existence of a third class of events in minimum bias pp collisions characterised by the presence of one or very few clans, i.e., by the corresponding NBD parameter $k_{th} < 1$, has been examined in pseudo-rapidity intervals accessible at LHC ($|\eta| < 0.9$) paying attention to total charged particle multiplicity distributions, forward-backward multiplicity correlations and energy density. Assuming that the guesswork at the basis of our calculations will be confirmed, more than try to draw conclusions one should ask two intriguing questions for future experimental and theoretical work:

1. what new physical phenomenon is hidden behind the squeezing of one or very few clans in the rapidity interval $|\eta| < 0.9$ with much stronger forward-backward multiplicity correlations than the soft and semi-hard components, and with energy density comparable with that of nucleus-nucleus at RHIC?

2. what would be the QCD counterpart of this new phenomenon? would it be a signal of parton saturation?

References

1. A. Giovannini, R. Ugoccioni, Phys. Rev. D, **68**, 034009 (2003)
2. A. Giovannini, R. Ugoccioni, Phys. Rev. D **60**, 074027 (1999)
3. A. Giovannini, L. Van Hove, Z. Phys. C **30**, 391 (1986)
4. A. Giovannini, R. Ugoccioni, Phys. Rev. D **59**, 094020 (1999)
5. A. Giovannini, R. Ugoccioni, Phys. Rev. D **66**, 034001 (2002)
6. D. Acosta et al. (CDF Collaboration), Phys. Rev. D **65**, 072005 (2002)
7. T. Alexopoulos et al. (E735 Coll.), Phys. Lett. **B435**, 453 (1998)
8. R.E. Ansorge et al. (UA5 Collaboration), Z. Phys. C **43**, 357 (1989)
9. T. Sjöstrand et al., Comput. Phys. Commun. **135**, 238 (2001)
10. J.D. Bjorken, Phys. Rev. **D27**, 140 (1983)